

Improving STAP Performance in Bistatic Space-Based Radar Systems using an efficient Expectation-Maximization Technique

Douglas A. Page, BAE Systems, Burlington, Massachusetts
Braham Himed, AFRL/SNRT, Rome, New York
Mark E. Davis, AFRL/SNRT, Rome, New York

Key Words: Space-based radar, bistatic radar, STAP, expectation-maximization, knowledge-aided STAP

SUMMARY & CONCLUSIONS

In this paper, we describe a space-time adaptive processing (STAP) approach for bistatic space-based radar (SBR) systems. A candidate SBR system employing a transmitter at medium earth orbit (MEO) and an airborne receiver is defined. A STAP configuration for performing wide area ground moving target indication (GMTI) is also specified. STAP performance is analyzed using simulated data in two different bistatic SBR geometries. Standard STAP performance degradation is shown to be a function of the relative severity of clutter non-stationarity in the two scenarios. To provide enhanced estimation of the clutter statistics, we apply an approach based on an efficient form of an expectation-maximization (EM) algorithm for estimating covariance matrices in non-stationary interference. The STAP performance of the EM technique is compared to that of standard STAP processing and higher order Doppler warping. The EM approach is seen to produce a usable Doppler space fraction (USDF) that is significantly improved over the other techniques. It has several powerful features, including the ability to align non-linear angle-Doppler contours, adaptivity to interference without applying a fixed range-dependent transformation, and the ability to simultaneously compensate for different range dependencies in higher range and Doppler ambiguities. The EM STAP approach also naturally accommodates knowledge-aided STAP techniques that improve understanding of clutter reflectivity variations.

1. INTRODUCTION

A bistatic, space-based radar (SBR) system is a promising concept for affordable wide-area ground moving target indication (GMTI) surveillance [1, 2]. The bistatic geometry allows the range to the receiver to be much smaller than the range from the transmitter, thus reducing the transmit power and antenna size required to detect ground targets. Employing a medium earth orbit (MEO) transmitter allows coverage of the entire earth with only a small number of satellites [3].

Due to unique clutter characteristics, however, challenges exist for performing space-time adaptive processing (STAP) to separate slowly moving targets from interference in these

systems. The large satellite velocities of space-based platforms produce a wide spread in clutter Doppler frequency compared to airborne radar platforms, producing endo-clutter conditions for a wider range of target velocities than for airborne GMTI systems. As described in [4, 5], in a bistatic radar system there is significant angle-Doppler dispersion of the clutter returns. This produces a geometry-induced range dependence to the clutter covariance matrix, making estimation of the clutter statistics more difficult. Moreover, the clutter ridge is non-linear, thus making the rank of the covariance matrix larger than in a monostatic radar system. The effects of bistatic geometry have been found to cause significant STAP degradation in bistatic airborne radar systems [4-6].

Specialized techniques have already been developed for producing improved covariance estimates in airborne bistatic geometries. These include higher order Doppler warping (HODW) [7], derivative based updating (DBU) [8], and angle-Doppler compensation (ADC) [4]. HODW applies a range-dependent Doppler shift in order to compensate for clutter non-stationarity. DBU relies on a Taylor series expansion of the STAP weight vector as a function of range. The ADC technique [4] improves on HODW by incorporating both a temporal and a spatial shift into the range-dependent transformations.

In order to address the unique challenges presented by bistatic SBR GMTI systems, we modified the expectation-maximization (EM) algorithm [9] and applied it to bistatic radar data. The technique incorporates model-based range-dependent clutter covariance matrices into calculation of STAP filter weights. The EM procedure performs iterative, maximum-likelihood estimation of a range-independent residual covariance matrix. Clutter nonstationarity is accounted for by incorporating knowledge of the geometry-induced range variation of the clutter into the model-based covariance matrices. Robustness is built into the EM procedure, as any errors in the model-based covariances will enter into the residual covariance estimate (modeled as stationary), and thus be corrected for when the STAP filter weights are computed. Effects such as range-dependent non-linearity of the angle-Doppler contours, terrain height-induced

Report Documentation Page

Form Approved
OMB No. 0704-0188

Public reporting burden for the collection of information is estimated to average 1 hour per response, including the time for reviewing instructions, searching existing data sources, gathering and maintaining the data needed, and completing and reviewing the collection of information. Send comments regarding this burden estimate or any other aspect of this collection of information, including suggestions for reducing this burden, to Washington Headquarters Services, Directorate for Information Operations and Reports, 1215 Jefferson Davis Highway, Suite 1204, Arlington VA 22202-4302. Respondents should be aware that notwithstanding any other provision of law, no person shall be subject to a penalty for failing to comply with a collection of information if it does not display a currently valid OMB control number.

1. REPORT DATE 01 MAY 2005		2. REPORT TYPE N/A		3. DATES COVERED -	
4. TITLE AND SUBTITLE Improving STAP Performance in Bistatic Space-Based Radar Systems using an efficient Expectation-Maximization Technique				5a. CONTRACT NUMBER	
				5b. GRANT NUMBER	
				5c. PROGRAM ELEMENT NUMBER	
6. AUTHOR(S)				5d. PROJECT NUMBER	
				5e. TASK NUMBER	
				5f. WORK UNIT NUMBER	
7. PERFORMING ORGANIZATION NAME(S) AND ADDRESS(ES) BAE Systems, Burlington, Massachusetts				8. PERFORMING ORGANIZATION REPORT NUMBER	
9. SPONSORING/MONITORING AGENCY NAME(S) AND ADDRESS(ES)				10. SPONSOR/MONITOR'S ACRONYM(S)	
				11. SPONSOR/MONITOR'S REPORT NUMBER(S)	
12. DISTRIBUTION/AVAILABILITY STATEMENT Approved for public release, distribution unlimited					
13. SUPPLEMENTARY NOTES See also ADM002017. Proceedings of the 2005 IEEE International Radar Conference Record Held in Arlington, Virginia on May 9-12, 2005. U.S. Government or Federal Purpose Rights License., The original document contains color images.					
14. ABSTRACT					
15. SUBJECT TERMS					
16. SECURITY CLASSIFICATION OF:			17. LIMITATION OF ABSTRACT	18. NUMBER OF PAGES	19a. NAME OF RESPONSIBLE PERSON
a. REPORT unclassified	b. ABSTRACT unclassified	c. THIS PAGE unclassified			

non-stationarity, and different range-dependencies in multiple ambiguities can all be incorporated into the model-based covariance matrices. This makes the EM-STAP technique a powerful approach for attaining low minimum detectable velocity (MDV) with bistatic SBR GMTI systems.

We evaluated the EM approach in two bistatic SBR scenarios using simulated radar data and compared the signal to interference plus noise ratio (SINR) loss curves to those of standard STAP techniques. While HODW was observed to provide significant benefits over standard STAP approaches, the EM approach was seen to provide substantial further improvements, yielding a usable Doppler space fraction (USDF) close to that of ideal processing.

2. BISTATIC SBR SYSTEM AND SCENARIO DEFINITION

Reference [3] defined the requirements and challenges for a space-based radar (SBR) system meeting the need for wide area surveillance of ground targets. These requirements form the basis for the driving parameters assumed in this paper and summarized in Table 1. In [2, 10], the design of a bistatic SBR system employing a space-based transmitter and airborne receiver for GMTI surveillance was considered. The radar system parameters shown in Table 1 reflect a modification of the design presented in [10], corresponding to a MEO rather than a low earth orbit (LEO) transmit platform.

A wide range of geometries may be encountered in a bistatic SBR system, depending on the locations of the transmit and receive platforms relative to the target, as well as the different possible orientations of the transmit and receive velocity vectors. One important quantity characterizing the geometry is the bistatic angle, defined as the angle between the line of sight from the center of the transmit beam to the transmitter and the line of sight to the receiver. In this paper we considered two different geometries:

- 1) A “90° bistatic angle” geometry in which the bistatic angle is approximately 90°.
- 2) A “pseudo-monostatic” geometry in which the bistatic angle is close to 0°.

TABLE 1. PARAMETERS OF ASSUMED BISTATIC SBR SYSTEM

Mission	Ground moving target indication (GMTI)
Target radar cross section	10 m ² , independent of aspect
Coverage rate	250 km by 250 km every 10 sec
Transmitter altitude	10,000 km (MEO)
Transmitter grazing angle	10-60 degrees
Radar frequency	5.4 GHz (C-band)
Transmit antenna size	50 m by 20 m
Average power	3 kW
CPI	45 ms
PRF	1 kHz
Receive altitude	20 km
Receive platform speed	200 m/s
Receive antenna size	2 m by 0.5 m
Antenna configuration	36 vertical subarrays

Table 2 summarizes the parameters for these two scenarios. Note that the 4.8° receive grazing angle corresponds to

approximately a 200 km range from the receiver to the target position.

Table 2. Simulated bistatic scenario parameters

	Scen. #1	Scen. #2
Look direction of transmitter at target location	West	North
Grazing angle to transmitter at target location	23°	23° deg
Heading of transmit ground track	South	East
Look direction of receiver at target location	North	North
Grazing angle to receiver at target location	4.8°	4.8°
Heading of receive ground track	West	East
3D Bistatic angle	88.1°	18.7°
Transmit footprint area	1000 km ²	1000 km ²

In order to simulate the effects of bistatic SBR clutter, ground locations within each bistatic range-gate were determined. Each range-gate corresponds to a time of arrival surface, which is an ellipsoid with foci at the transmit and receive locations. The intersection of the range ellipsoids with the earth’s surface (assumed spherical) define the locations of ground clutter scatterers in each range-gate.

For each scenario, 3 range ambiguities of ground clutter returns were simulated. Figures 1 and 2 show the visible portions of the ambiguities for scenarios 1 and 2, respectively on a latitude-longitude display. The receive platform location and transmit antenna footprint are also shown. Note that the higher range ambiguities are well outside the antenna footprint, which results in attenuated returns from the ambiguities.

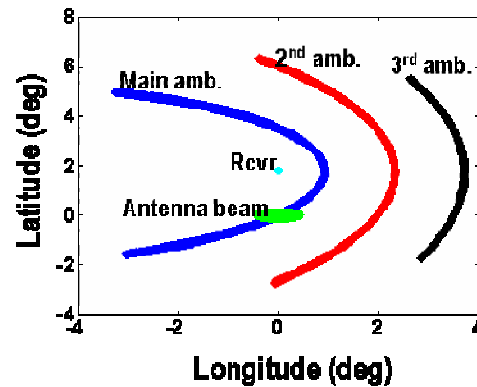


Figure 1 Visible portions of 3 range ambiguities, scenario #1

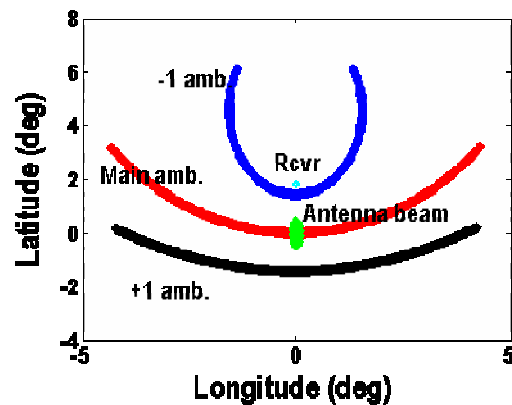


Figure 2 Visible portions of 3 range ambiguities, scenario #2

3. STANDARD STAP PERFORMANCE

Complex radar returns from the clutter scatterers in each bistatic range-gate were simulated and used to evaluate the performance of different STAP techniques. The return amplitudes of the scatterers were calculated using the bistatic radar range equation, while the spatial responses across the receive antenna subarrays were calculated assuming far-field plane wave returns. The temporal responses of the scatterers across the pulses within the coherent processing interval (CPI) were determined by calculating the total Doppler frequency due to the transmitter and receiver radial velocity and earth rotation. The effects of earth rotation and frequency dispersion across the 18 MHz bandwidth were found to have a significant impact on STAP performance.

Earth rotation causes a modification of the angle-Doppler clutter ridge, due to the radial velocity components of earth rotation towards the transmit and receive platforms at the ground scatterer positions. Frequency dispersion broadens the clutter ridge, due to the appearance of the radar wavelength in the denominator of the expression for the scatterer phase on a given channel and pulse. This broadening increases with the displacement of the clutter ridge from zero spatial and temporal frequency, and widens the filter null required to mitigate the ground clutter.

In order to mitigate frequency dispersion, time delay steering (TDS) on the antenna subarrays was employed to shift the spatial and temporal frequency to zero at the center of the antenna footprint. Figure 3 shows the SINR loss in scenario #1 as a function of Doppler frequency for ideal STAP processing (i.e. using the ideal covariance matrix for all 36 spatial and 45 temporal degrees of freedom (DOF)), with and without TDS. The effect of TDS is seen to be a shift of the clutter null to zero Doppler frequency. The clutter null is also seen to be narrowed significantly by TDS, due to the reduction of the effects of frequency dispersion on the clutter returns.

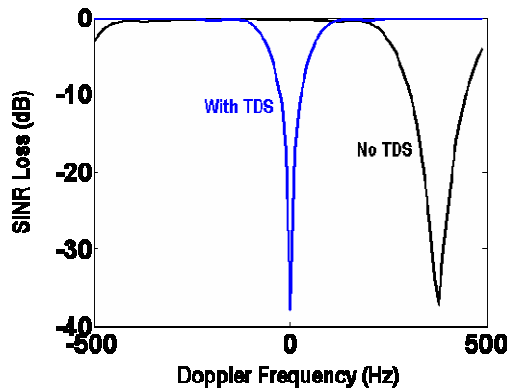


Figure 3 Scenario #1 SINR loss as a function of target Doppler frequency for ideal STAP processing without (black) and with (blue curve) time delay steering (TDS) of the antenna subarrays on each pulse

In order to limit the size of the training window used to estimate the covariance matrix for STAP processing, reduction of the number of DOFs is essential. We found PRI-staggered post-Doppler processing [11] to be the most effective temporal

DOF reduction technique in the bistatic SBR scenarios considered. Figure 4 shows STAP performance for scenario #1 using ideal reduced-DOF covariance matrices for 1 and 2 staggers compared to full-DOF processing. No spatial DOF reduction is present, so the total number of DOFs is equal to 72 (36 spatial subarrays times 2 temporal staggers). Due to the angle-Doppler correlation of the clutter returns, employing only 1 stagger, which is equivalent to post-Doppler adaptive spatial processing only, is clearly inadequate. It appears, however, that employing 2 pulse staggers gives performance that is nearly as good as ideal, full-DOF processing. We thus used PRI-staggered post-Doppler processing with 2 staggers in all our STAP performance calculations.

We consider two different sets of spatial DOFs in this paper: a) All 36 subarrays (i.e. “element-space”) and b) beam-space processing using 5 beams centered at the target direction. Element-space processing maximizes the number of adaptive degrees of freedom available for mitigating ground clutter, jamming, and other types of interference such as weather clutter. Beam-space processing provides fewer adaptive DOFs for interference mitigations, but allows the use of smaller training windows for covariance estimation, thus minimizing the effects of clutter nonstationarity.

STAP performance for the two DOF sets described above was calculated using estimated clutter covariance matrices obtained by averaging over training range-gates surrounding the target test cell. The training window for element-space processing was selected as twice the number of DOFs (72 range-gates on either side of the target range-gate, for a total of 144 training samples). The training window for beam-space processing was selected as three times the number of DOFs (15 range-gates on either side of the target range-gate, for a total of 30 training samples). Radar data vectors were generated for all the training range-gates in each scenario and used to determine estimated covariance matrices and STAP performance in each scenario. Figure 5 shows the resulting SINR loss versus Doppler frequency, averaged over 10 realizations. For reference, the full-DOF ideal SINR loss curve is also shown.

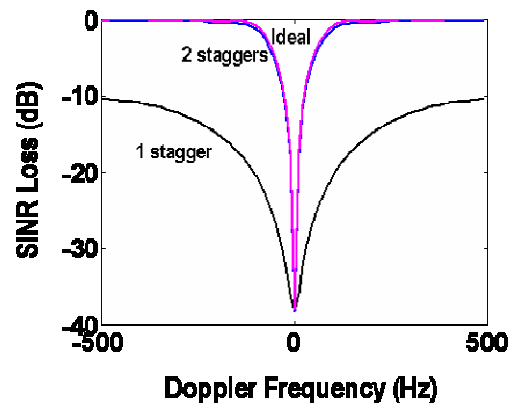


Figure 4 SINR loss as a function of Doppler frequency using ideal covariance matrices for PRI-staggered post-Doppler STAP with 1 and 2 pulse staggers. The performance of full-DOF ideal STAP processing is also shown.

Note the large degradation in SINR loss of element-space processing in scenario #1 compared to ideal STAP processing. In this scenario beam-space processing, with the smaller required number of training samples, is seen to perform much better than element-space, but is still significantly degraded relative to ideal processing.

Observe that the element-space SINR loss curves are seen to be more degraded in scenario #1 relative to scenario #2. This behavior can be understood by comparing the dispersion of the clutter spectral center [4], which is defined as the location of the peak clutter spectrum along a range contour. Since STAP performance is a function of clutter angle-Doppler clutter characteristics, we examined the locations of the clutter spectral centers in angle-Doppler space. Figure 6 shows a portion of the normalized angle-Doppler contours, for the range cells at either end of the 144 range-gate training window, as well as the test range cell.

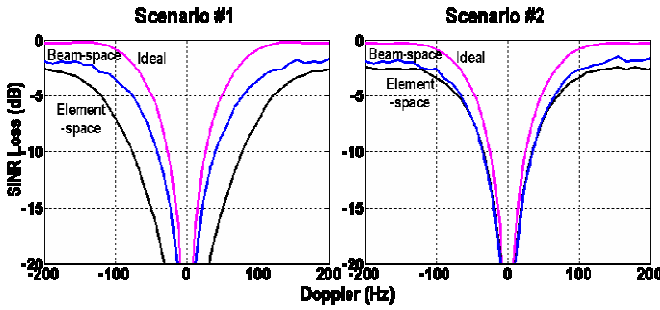
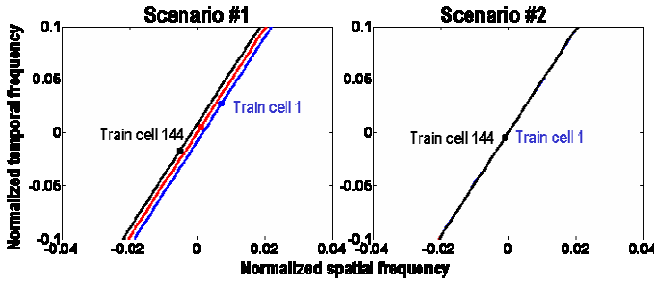


Figure 5 SINR loss as a function of Doppler frequency in scenarios #1 (left) and #2 (right) for a) ideal, full-DOF STAP (top, magenta curve) b) beam-space PRI-staggered post-Doppler STAP with 10 DOFs and a 30 range-cell training window (middle, blue curve) and c) element-space PRI-staggered post-Doppler STAP 72 DOFs and a 144 range-cell training window (bottom, black curve).



(a) scenario # 1 (b) scenario # 2

Figure 6 Portion of normalized angle-Doppler trajectories for 3 range-gates (training window ends and test cell)

The variation of the spectral center locations across the training window can be clearly seen in scenario #1. This variation indicates that estimation errors will occur after averaging over training range-gates to obtain covariance matrix estimates. Note that there appears to be no discernable range variation of the angle-Doppler clutter ridge and spectral centers in scenario #2. This is due to the pseudo-monostatic

geometry, and causes reduced estimation errors. This explains the improved element-space STAP performance observed in the pseudo-monostatic scenario compared to the 90 degree bistatic angle scenario.

4. AN EFFICIENT EM ALGORITHM FOR BISTATIC SBR STAP

Reference [9] defined a method for estimating covariance matrices in the presence of non-stationary interference. We briefly review this technique here and then describe the modification we made to improve processing efficiency. We then describe application to bistatic SBR STAP, and in the next section present the results we obtained in the two simulated scenarios.

In the technique of Ref. [9], the space-time data vector in each range-gate k is modeled as the sum of two terms:

$$\mathbf{x}(k) = \mathbf{x}_1(k) + \mathbf{x}_2(k), \quad (1)$$

$$\langle \mathbf{x}_1(k) \mathbf{x}_1^H(k) \rangle \equiv \mathbf{R}_1 \quad \langle \mathbf{x}_2(k) \mathbf{x}_2^H(k) \rangle \equiv \mathbf{R}_2(k)$$

The stationary term is assumed to be a complex, zero mean circular Gaussian random variable, with a range independent covariance \mathbf{R}_1 that is to be estimated. An initial estimate of \mathbf{R}_1 is assumed to be available. The non-stationary term is also assumed to be a complex, zero mean circular Gaussian, but has a known covariance $\mathbf{R}_2(k)$ that varies with range.

If the stationary data vector components were known, a maximum likelihood estimate of \mathbf{R}_1 could easily be obtained. Even though these components are unknown, their probability density function (pdf), conditioned on the full data vectors $\mathbf{x}(k)$ and the current estimate $\mathbf{R}_1^{(q)}$, is known (q is the current iteration index). The expectation value of the maximum likelihood estimate of \mathbf{R}_1 can be computed using this conditional pdf. The result, which is equivalent to Eq. (3.4) of [9], is used as the updated estimate of \mathbf{R}_1 on iteration $(q+1)$:

$$\mathbf{R}_1^{(q+1)} = \mathbf{R}_1^{(q)} + \mathbf{R}_1^{(q)} \frac{1}{K} \sum_{k=1}^K \left\{ \mathbf{y}(k) \mathbf{y}^H(k) - \left[\mathbf{R}_1^{(q)} + \mathbf{R}_2(k) \right]^{-1} \right\} \mathbf{R}_1^{(q)},$$

$$\mathbf{y}(k) = \left[\mathbf{R}_1^{(q)} + \mathbf{R}_2(k) \right]^{-1} \mathbf{x}(k), \quad (2)$$

where K is the number of training range-gates used.

The technique described above involves a substantial amount of processing, due to the matrix inversions that are required in each training cell k and on each iteration. We developed a modification to the procedure in order to reduce the processing load. The estimates of the stationary covariance matrix on two successive iterations are assumed to be related by

$$\mathbf{R}_1^{(q+1)} = \mathbf{R}_1^{(q)} + \nu \mathbf{v}^H, \quad (3)$$

where ν represents the updated knowledge of the stationary interference on the current iteration.

The mean value of the log-likelihood function of the stationary interference components is next computed using the same conditional pdf used to derive Eq. (2). The vector \mathbf{v} that maximizes the mean log-likelihood is then found. The solution reduces to the eigenvalue problem

$$\mathbf{M}\mathbf{v} = \lambda_{\max} \mathbf{v} \quad (4)$$

The matrix \mathbf{M} is given by the equation

$$\mathbf{M} = K \cdot \mathbf{I} + \mathbf{R}_1^{(q)} \left\{ \mathbf{y}(k) \mathbf{y}^H(k) - [\mathbf{R}_1^{(q)} + \mathbf{R}_2(k)]^{-1} \right\}, \quad (5)$$

where \mathbf{I} is the identity matrix. The vector \mathbf{v} is thus proportional to the eigenvector of \mathbf{M} having the largest eigenvalue. The proportionality constant is determined using

$$\mathbf{v}^H [\mathbf{R}_1^{(q)}]^{-1} \mathbf{v} = \alpha \cdot \left(\frac{\lambda_{\max}}{K} - 1 \right) \quad (6)$$

Technically, $\alpha=1$ provides the exact solution to the maximization problem. However, a value $\alpha < 1$ is desirable to improve convergence of the algorithm.

The modified procedure just described reduces the processing requirements, because the matrix inverses can be updated using the following matrix inversion lemma:

$$(\mathbf{R} + \mathbf{v}\mathbf{v}^H)^{-1} = \mathbf{R}^{-1} - \frac{\mathbf{R}^{-1}\mathbf{v}\mathbf{v}^H\mathbf{R}^{-1}}{1 + \mathbf{v}^H\mathbf{R}^{-1}\mathbf{v}} \quad (7)$$

Thus, the matrix inverses need be computed only on the first iteration. Once they are computed, they can be updated on successive iterations using the above formula.

Once the EM iterations have been completed, the STAP weight vector in the test cell k_0 is then computed using

$$\mathbf{w} = [\mathbf{R}_1^{(Q)} + \mathbf{R}_2(k_0)]^{-1} \mathbf{s}_t, \quad (8)$$

where Q is the last iteration index and \mathbf{s}_t is the target steering vector. This weight vector is then used to perform adaptive filtering.

To apply this technique to the bistatic SBR problem, we computed the non-stationary covariance matrices using

$$\mathbf{R}_2(k) = A \sum_i \mathbf{s}_i \mathbf{s}_i^H \quad (9)$$

Here, i is an index labelling a set of point scatterers along the bistatic clutter ridge. A constant receive azimuth spacing of the scatterers is assumed in each bistatic range-gate, and a separate set of point scatterers is defined in each Doppler filter. If range or Doppler ambiguities are expected to produce significant returns, point scatterers may also be defined in these ambiguities. This allows compensation for the different amounts of clutter range variation in each range and Doppler ambiguity producing significant returns.

For the results shown in the next section, the amplitude A of the scatterers was assumed to be a constant. However, if knowledge-aided processing was being employed, the amplitude could be varied with range and azimuth based on knowledge of the terrain conditions. This would be expected to produce significant benefits in nonhomogeneous terrain conditions.

To determine the post-Doppler space-time steering vectors \mathbf{s}_i of the scatterers, their spatial and temporal frequencies were computed using knowledge of the platform parameters and terrain elevation. Note that these frequencies are generally located on a nonlinear angle-Doppler contour. This allows, for example, compensation for a range-dependent mismatch of both the slope and location of the angle-Doppler contours.

The fact that the EM technique adaptively estimates a stationary covariance matrix implies that it can adaptively estimate interference that is not due to ground clutter (such as jamming or rain clutter). Moreover, it does this without introducing any modulation of that interference. Such modulation would occur, for example, when a range-dependent Doppler shift is applied to the radar data during HODW processing. This added modulation is range-dependent and thus may degrade the estimation of interference not due to ground clutter.

5. PERFORMANCE COMPARISON

The efficient EM procedure described above was applied to the two bistatic SBR scenarios with the parameter values $A=20$, $Q=20$, $\alpha=0.25$. Figure 7 shows the resulting SINR loss as a function of Doppler frequency along with the performance of ideal STAP, standard element-space and beam-space STAP, and HODW in scenarios 1 and 2. Both EM and HODW were implemented in the element-space, PRI-staggered configuration with 72 DOFs.

The USDF for a -5 dB SINR loss threshold for each algorithm was also computed and is shown for each scenario (this threshold corresponds to approximately a 15 dB SINR for the candidate system).

In scenario #1, while HODW shows a significant benefit over standard element-space processing, EM provides a further improvement of 3.6% in USDF, yielding a value within 1% of the ideal STAP USDF. In scenario #2, standard processing performs much better than in scenario #1 as was seen in section 3. In this scenario only the EM technique is seen to provide additional improvement over element-space STAP processing. These results indicate that the EM STAP approach described in this paper may be a promising technique for mitigating non-stationary clutter in bistatic SBR systems. Further evaluations are underway to investigate performance and robustness in different geometries and in the presence of weather clutter. Combination with knowledge-aided STAP processing under non-homogeneous, real-world terrain conditions is also being investigated.

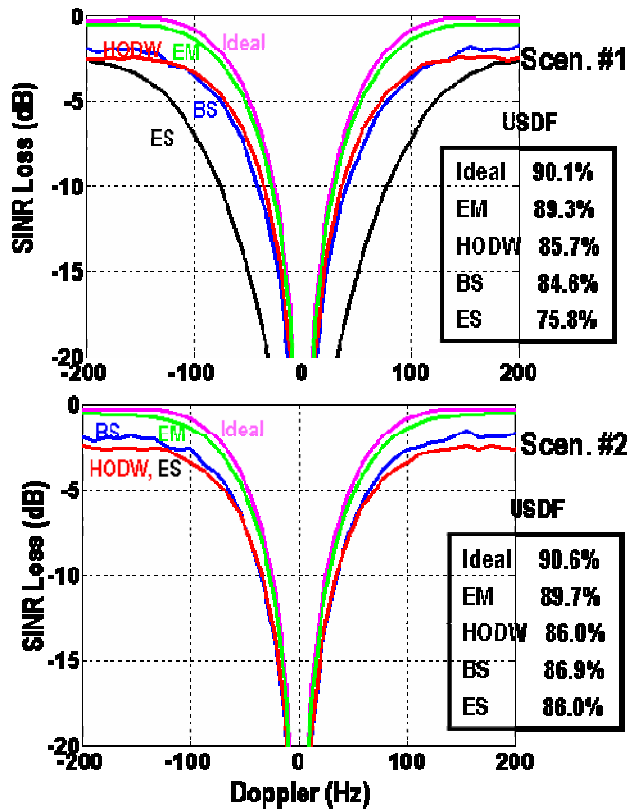


Figure 7 SINR loss as a function of Doppler frequency in scenario #1 (top plot) and #2 (bottom plot) for a) ideal STAP (magenta, top curve) b) EM STAP processing (green, second from top) c) HODW (red curve) d) standard beam-space STAP (BS, blue curve) and e) standard element-space STAP (ES, black curve). Usable Doppler space fraction (USDF) is shown for each algorithm.

REFERENCES

- [1] G. L. Guttrich, W. E. Sievers, and N.M. Tomljanovich, "Wide Area Surveillance Concepts Based on Geosynchronous Illumination and Bistatic Unmanned Airborne Vehicles or Satellite Reception", Proceedings of the 1997 IEEE National Radar Conference, pp. 126-131
- [2] Michael P. Harnett and Mark E. Davis, "Bistatic Surveillance Concept of Operations", Proceedings of the 2001 IEEE National Radar Conference, pp. 75-80
- [3] M.E. Davis, "Space Based Radar Core Technology Challenges for Affordability", 2001 Core Technologies for Space Systems Conference, Colorado Springs, Colorado, Nov. 28-30, 2001
- [4] B. Himed, Y. Zhang, and A. Haijari, "STAP with Angle-Doppler Compensation for Bistatic Airborne Radars", Proceedings of the 2002 IEEE Radar Conference, pp. 311-317
- [5] Braham Himed, James H. Michels, and Yuhong Zhang, "Bistatic STAP Performance Analysis in Radar Applications", Proceedings of the 2001 IEEE National Radar Conference, pp. 198-203

- [6] William L. Melvin, Michael J. Callahan, and Michael C. Wicks, "Bistatic STAP: Application to Airborne Radar", Proceedings of the 2002 IEEE Radar Conference, pp. 1-7
- [7] F. Pearson and G. Borsari, "Simulation and Analysis of Adaptive Interference Suppression for Bistatic Surveillance Radars", 9th Annual Adaptive Sensor Array Processing Workshop, 13-14 March 2001
- [8] Michael Zatman, "Performance Analysis of the Derivative Based Updating Method", 9th Annual Adaptive Sensor Array Processing Workshop, 13-14 March 2001
- [9] D. R. Fuhrmann, "Covariance Estimation in Non-stationary Interference", 1993 Signals, Systems, and Computers Asilomar Conference, pp. 1172-1175
- [10] Michael P. Harnett and Mark E. Davis, "Operations of an Airborne Bistatic Adjunct to Space Based Radar", Proceedings of the 2003 IEEE National Radar Conference, pp. 133-138
- [11] J. Ward, "Space-Time Adaptive Processing for Airborne Radar", Tech. Rep. F19628-95-C-0002, MIT Lincoln Laboratory, December 1994

BIOGRAPHIES

Douglas Page is a lead engineer at BAE Systems, Advanced Information Technologies in Burlington, MA. He received his B.S. (1983), M. Eng. (1984) and Ph.D. (1992) degrees from Rensselaer Polytechnic Institute in Troy, N.Y. He has over 10 years experience in radar signal processing and is currently developing STAP techniques for airborne and space-based GMTI radar applications. Dr. Page is a member of Tau Beta Pi, Eta Kappa Nu, and Sigma Xi.

Braham Himed is a senior research engineer with the United States air force research Laboratory, sensors directorate. He received his B.S. degree from Ecole Nationale Polytechnique of Algiers, Algeria in 1984, and his M.S. and Ph.D. degrees from Syracuse University, Syracuse, NY, in 1987 and 1990, respectively, all in Electrical Engineering. His research interests include detection, estimation, multichannel adaptive signal processing, time series analyses, array processing, space-time adaptive processing, hot clutter mitigation, and ground penetrating radar technology. Dr. Himed is a senior member of the IEEE and a member of the radar systems panel.

Mark E. Davis is the Principal Engineer – Radar Systems for Air Force Research Laboratory, Sensors Directorate. He has responsibility within AFRL for the coordinating the technical and investment strategy for future Space Based Radar capabilities. He has Thirty-two years experience in engineering and program management of microwave and radar for surveillance and fire control systems. His education includes a PhD in Physics from the Ohio State University and a Master in Electrical Engineering from Syracuse University. He is a Senior Member of the IEEE, and a member of the Radar Panel of the Aerospace Electronics Systems Society.